



## Green Synthesis and Characterization of Crystalline CuO Nanoparticles using Aqueous Mentha Piperita L. Leaf Extract

\*Fatma A. Shtewi, Wedad M. Al-Adiwish, Hamid A. Alqamoudy, and Awatif A. Tarroush

Chemistry Department, Faculty of Science, Zawia University, Libya

### Keywords:

Copper oxide nanoparticles  
Green synthesis  
Mentha Piperita L.  
Polyphenols  
X-ray diffraction

### ABSTRACT

Copper oxide nanoparticles are essential technology materials that are utilized as catalysts in the chemical industry, as well as in photonic and electronic devices and medical applications. Due to their applications in advanced technologies, we have concentrated on the production of CuO nanoparticles using enhanced, cost-effective, and environmentally friendly synthetic techniques. In this paper, we have presented a green synthesis technique to successfully synthesis copper oxide nanoparticles (CuO NPs) utilizing copper (II) sulfate pentahydrate (CuSO<sub>4</sub>.5H<sub>2</sub>O) as precursor salt and Mentha Piperita leaf extract as a reducing and stabilizing agent during the synthesis process. The precursor salt solution and reducing agent were mixed in a 1:1 volume ratio at 50 °C. The CuO NPs synthesized were confirmed by the characteristics Surface Plasmon Resonance (SPR) peak in the UV-visible region. Also, the optical direct band gap energy of the CuO NPs determined from the Tauc plot was 3.26 eV. The FTIR spectrum analysis confirmed existence of functional groups of polyphenols from Mentha piperita L. leaf extract, which are responsible for the reduction of Cu<sup>2+</sup> ions and effective stabilization of CuO NPs. All the peaks observed in the XRD pattern revealed the production of CuO NPs having monoclinic structure with an average crystallite size of 42.51 nm. The surface morphology of the CuO nanoparticles was detected using SEM analysis. Further, the synthesis mechanism of CuO NPs has also been investigated.

## الاصطناع الأخضر والتشخيص لجسيمات CuO النانوية البلورية باستخدام المستخلص المائي لأوراق النعناع

\*فاطمة على الشتيوي و وداد ميلاد الابدويش و حامد أبو عجيلة القمودي و عواطف عبدالسلام طروش

قسم الكيمياء، كلية العلوم، جامعة الزاوية، ليبيا

### الكلمات المفتاحية:

جسيمات أكسيد النحاس النانوية  
الاصطناع الأخضر  
النعناع  
البوليفينولات  
حيود الأشعة السينية.

### المخلص

تعتبر جسيمات أكسيد النحاس النانوية من المواد التكنولوجية الهامة المستخدمة كمحفزات في الصناعات الكيميائية وكذلك في الأجهزة الفوتونية والإلكترونية والتطبيقات الطبية. نظراً لتطبيقاتها المتقدمة، فقد ركزنا على إنتاج الجسيمات النانوية لـ CuO مع استراتيجيات تركيبية محسنة وفعالة من حيث التكلفة وصديقة للبيئة. في هذا البحث، قدمنا تقنية تخليق خضراء لتصنيع جسيمات أكسيد النحاس النانوية (CuO NPs) بنجاح باستخدام كبريتات النحاس المائية (CuSO<sub>4</sub>.5H<sub>2</sub>O) كملح أولي ومستخلص أوراق النعناع كعامل مختزل ومثبت أثناء عملية الاصطناع. تم خلط محلول الملح الأولي وعامل الاختزال بنسبة حجمية 1:1 عند 50 درجة مئوية. تم تأكيد اصطناع الجسيمات النانوية لـ CuO من خلال نطاق امتصاص رنين البلازمون السطحي (SPR) في المنطقة المرئية للأشعة فوق البنفسجية. أيضاً كانت طاقة فجوة النطاق البصري المباشر لـ CuO NPs المحددة من مخطط Tauc 3.26 إلكترون فولت. أكد تحليل طيف FTIR وجود مجموعات وظيفية للبوليفينولات من مستخلص أوراق النعناع، المسؤولة عن إختزال أيونات النحاس (II) والتثبيت الفعال لجسيمات أكسيد النحاس النانوية. كشفت جميع القمم التي لوحظت في نمط XRD عن تكوين CuO NPs ذات بنية أحادية الميل

\*Corresponding author:

E-mail addresses: [f.shtewi@zu.edu.ly](mailto:f.shtewi@zu.edu.ly), (W. M. Al-Adiwish) [w.aladiwish@zu.edu.ly](mailto:w.aladiwish@zu.edu.ly), (H. A. Alqamoudy) [hamed\\_alqamoudy@zu.edu.ly](mailto:hamed_alqamoudy@zu.edu.ly), (A. A. Tarroush) [a.tarroush@zu.edu.ly](mailto:a.tarroush@zu.edu.ly)

Article History : Received 30 January 2021 - Received in revised form 27 June 2020 - Accepted 1 July 2021

مع متوسط حجم بلوري يبلغ 42.51 نانومتر. تم الكشف عن الشكل السطحي للجسيمات النانوية CuO باستخدام تحليل SEM. علاوة على ذلك، تمت مناقشة آلية اصطناع جسيمات أكسيد النحاس النانوية.

## 1. Introduction

Nanotechnology is an interdisciplinary and broad diverse field of research that has seen rapid growth worldwide in the past few years. Recent advancements in this subject have resulted in the production of metal and metal oxide nanoparticles. Particles with an average diameter of 1-100 nm are included [1]. Because of their small size, large surface area, chemical and optical properties, and good electrical conductivity, these particles are discovered to offer advantages. Among them, copper oxide nanoparticles (CuO NPs) have acquired great interest in research fields, such as high-Tc superconductors [2], solar cells [3], biodiesel [4], photocatalysis [5], supercapacitors [6], electrocatalysis [7], etc. due to their preferred characteristics such as nontoxicity and cheap cost. Moreover, CuO nanoparticles reveal a great potential for use as antimicrobial agents [8].

Several methods like thermal evaporation, sonochemical [9], sol-gel [10], hydrothermal [11], and electrochemical procedures [12] and microwave irradiation method [13] have all been used to produce copper oxide nanostructures with varied morphologies, dimensions and sizes using different physical, chemical, or combined physics and chemistry strategies. In contrast, nanoparticles synthesized using the above mentioned methods are suffering from drawbacks including, high reagent costs, hazardous reaction conditions, longer processing time and a time-consuming process to separate nanoparticles. Recently, there's scope to develop new methods for the production of metal and their metal oxide nanoparticles (M/MO NPs) which should be rapid, inexpensive, and environmentally friendly.

In recent years, green synthesis of copper oxide nanoparticles attracted much attention due to its nontoxicity and also being an economical and facile process. Polyphenolic compounds existing in the plant extracts are water soluble, nontoxic and biodegradable, playing a significant role during the green synthesis process [1]. The reported band gap energy ( $E_g$ ) values for CuO, which is a p-type semiconductor, are generally in the range of 1.2 to 2.16 eV. This wide range is caused by a variety of factors including, how the gap is interpreted (direct or indirect), grain size, annealing treatment, morphology, and doping. The favourable band gap energy of CuO around 2.6 eV makes it suitable for solar cell energy conversion and it can also be served as solar cell window material [14, 15].

In this work we are reporting the synthesis of CuO nanoparticles by reducing aqueous copper (II) sulfate pentahydrate solution by the extract of *Mentha piperita* leaves without the use of any dangerous and environmentally toxic chemicals involved previously in conventional chemical reduction methods. *Mentha piperita* (Lamiaceae family) contains a variety of phytochemicals including, polyphenols that have been shown to reduce of metal ions to their metal and metal oxide nanoparticles. The phytochemicals present in plant extracts also are highly effective antioxidants and are less toxic than the synthetic ones. Gallic acid, sinapic acid, and ellagic acid are the major phenolic chemicals found in *Mentha piperita* leaves. Also, *Mentha piperita* leaves extract contains a significant amounts of flavonoids (eriocitrin, narirutin, hesperidin, luteolin-7-O-rutinoside, isorhoifolin, diosmin, 5,7-dihydroxycromone-7-O-rutinoside), tannins and saponins [16]. The existence of hydroxyl groups in flavonoids makes them as a potent antioxidant. Dyab, A.S. [17] reported that fresh peppermint leaves extract contains higher values for total flavonoid (as Quercetine) and total phenolic (as Gallic acid). These compounds are responsible for the medicinal uses of *Mentha piperita* as antioxidant and antimicrobial agents.

## 2. Materials and Methods:

Fresh leaves of *Mentha piperita* plant were collected from farms in Az-Zāwiyah, Libya. Copper (II) sulfate pentahydrate ( $\text{CuSO}_4 \cdot 5\text{H}_2\text{O}$ ) and sodium hydroxide (NaOH) were obtained from the Sigma-Aldrich Company (Sigma-Aldrich, St Louis, MO, USA). These chemicals were utilized as supplied, with no further purification. All aqueous solutions were carefully prepared using distilled water.

### 2.1 Preparation of the plant extract:

20 g of *Mentha piperita* leaves were washed thoroughly with tap water then rinsed with distilled water until no foreign material remained. The leaves were finely cut and were boiled for 15 min with 100 ml of distilled water in 500-ml Erlenmeyer flask. The aqueous extract of *Mentha piperita* leaves was later filtered through cotton then through Whatman No.1 filter paper.

### 2.2 Synthesis of CuO nanoparticles:

In the present method, Copper (II) sulfate pentahydrate ( $\text{CuSO}_4 \cdot 5\text{H}_2\text{O}$ ) was used as basic precursor, *Mentha piperita* leaves extract as reducing and stabilizer agent. NaOH was used as a catalyst and also to adjust the pH to 9.

Copper oxide nanoparticles were synthesized by mixing (0.1 M)  $\text{CuSO}_4 \cdot 5\text{H}_2\text{O}$  solution as the precursor salt with *Mentha piperita* leaves extract in a 1:1 volume ratio. Then, the pH of the reaction mixture was adjusted to pH 9 by the addition of (0.1 M) NaOH, with rapid stirring at 50°C in a water bath. The reduction of copper sulfate to CuO Nps was confirmed by the color change of the solution from blue to greenish-black. The CuO nanoparticles were separated by centrifuging at 3000 rpm for 15 minutes and repeatedly washed by distilled water. Subsequently, the obtained precipitate was dried in the open air.

### 2.3 Characterization of CuO nanoparticles

The maximum optical absorption of the sample was characterized by UV-Visible spectrometer (JASCO V 670), in the wavelength range of 200-800nm. The UV-Vis data was used to calculate the band gap energy of the CuO NPs using Touch's plot method. Molecular vibrations analysis of the samples was performed by Fourier transform infrared spectroscopy (FT-IR). The samples were mixed with dry KBr, grounded and then pressed into thin pellets. The IR measurements were carried out on IRAffinity-1S (Shimadzu) spectrometer, with spectrum recorded in the wavenumber range of 500-4,000  $\text{cm}^{-1}$ . X-ray diffraction analysis (XRD) was used to confirm the crystal formation and to estimate the crystalline size of CuO NPs. The X-ray diffraction (XRD) measurements were performed using a Shimadzu 6100 XRD diffractometer, and the pattern was recorded with Copper K $\alpha$  radiation ( $\lambda=1.54060 \text{ \AA}$ ). The surface morphology and structural properties of the CuO nanoparticles were studied using scanning electron microscope (SEM).

## 3. Results and Discussions:

### 3.1 UV-Vis spectroscopy:

Reduction of aqueous copper ions by *Mentha piperita* leaves extract for the formation of copper oxide nanoparticles was first observed by color change from blue to greenish-black after the solution was made to pH 9 by the addition of (0.1M) NaOH and maintained at 50°C. Figure 1 shows the absorption spectra of *Mentha piperita* leaf extract and green synthesized CuO nanoparticles. Higher absorption peaks at the region 200 to 350 nm were observed for leaves extract. It indicates that the leaves extract had free phytochemicals. While a broad peak at the region between 200 nm and 400 nm was obtained from CuO nanoparticles most likely attributed to Surface Plasmon Resonance (SPR) of CuO semiconductor excitation. High absorbance indicates a high conversion of  $\text{Cu}^{2+}$  to CuO as nanoparticle leading to higher concentration of CuO NPs [18].

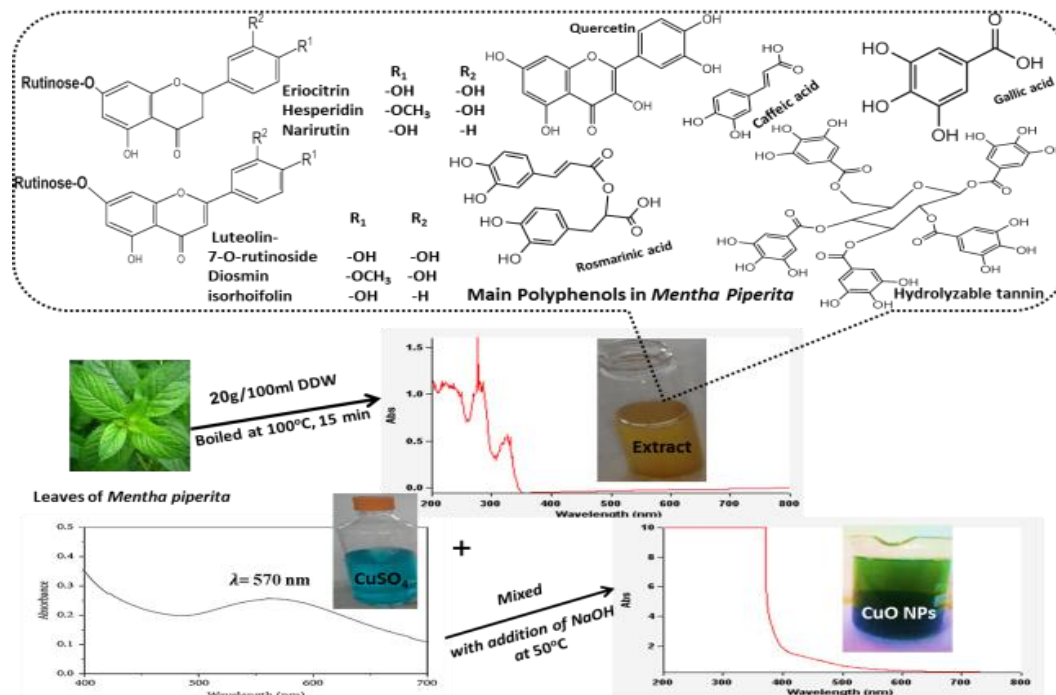
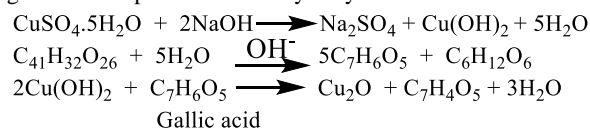
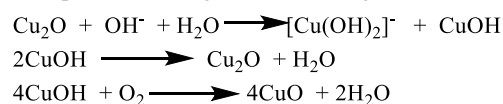


**Fig.1:** UV-visible absorption spectra of  $\text{CuSO}_4$ , *Mentha piperita* leaf extract and synthesized CuO nanoparticles.

The formation of CuO NPs was monitored by color changes. Tannins present in the *Mentha piperita* leaves extract playing a crucial role in the reduction process of  $\text{Cu}^{2+}$  ions. The changes in the color is also understood in terms of the chemical reaction between copper (II) sulfate pentahydrate and sodium hydroxide to produce copper (II) hydroxide (blue), which reacts with the gallic acid leading to the formation of dehydrogallic acid and copper(I) oxide (brown). The gallic acid is produced from hydrolysis of tannins.



However, as the reaction continues with time, copper (I) oxide was formed and at last CuO nanoparticles (greenish-black) formation takes place according to the following series of reactions [19].



### 3.2 Band gap energy:

Optical characteristics of nanoparticles provide valuable information about physical properties; such as band gap energy, band structure and optically active defects. The band gap ( $E_g$ ) value of the CuO nanoparticles has been studied. The absorption spectra can be used to estimate the energy gap of the produced NPs through Tauc's relation:

$$\alpha h\nu = A(h\nu - E_g)^{1/2}$$

Where  $\alpha$  is the absorption coefficient,  $A$  is constant related to the material,  $h\nu$  is the photon energy in eV,  $h$  is Planck's constant,  $\nu$  is the frequency of the photon,  $E_g$  is the optical band gap in eV. The energy band gap of the CuO nanoparticles was estimated by fitting a straight line to the linear portion of the curve and  $E_g$  is the intercept of the line with the  $h\nu$ -axis figure 2. The obtained direct band gap value was found to be 3.26 eV, which was lower than the bulk band gap value of CuO NPs (3.5 eV) [14]. The observed decrease in the direct band gap value could be ascribed to increasing particle size. Also, the energy gap decreases with increasing annealing temperature [20].

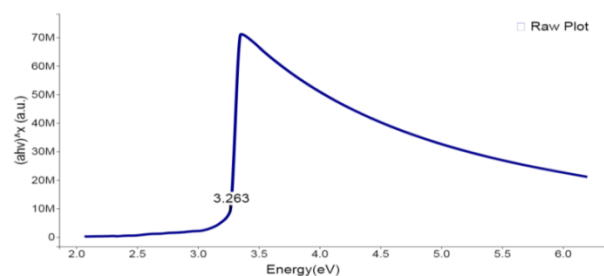


**Fig. 2:** Direct optical band gap energy of CuO nanoparticles.

### 3.3 FTIR spectroscopy

FT-IR measurements were employed to investigate the possible functional groups responsible for the reduction of the metal precursors and the formation of CuO NPs. The comparison between the IR spectrum of *Mentha piperita* powder and the IR spectrum of the product of its complexation with  $\text{Cu}^{2+}$  ions are shown in figure 3. The infrared spectra of the dried *M. piperita* leaves show absorption peaks at 1253.69 and 1014.85  $\text{cm}^{-1}$ , which can be ascribed for the C-O-C and C-O-H vibrations of the phenolic group. Also, the two small bands at 1416.17  $\text{cm}^{-1}$  and 1517.47  $\text{cm}^{-1}$  can be related to symmetric and asymmetric stretching vibrations of  $\text{COO}^-$  group. The band observed at 1601.29  $\text{cm}^{-1}$  is attributed to the C=C stretching vibrations of the aromatic ring, which belongs to the polyphenols (e.g., flavonoids and tannins) [21]. Moreover, the peak at 1730.08  $\text{cm}^{-1}$  corresponds to the C=O stretching vibration, which might arise from the functional groups of ketones, aldehydes, and carboxylic acids. The sharp peaks at 2919.45  $\text{cm}^{-1}$  and 2850.56  $\text{cm}^{-1}$  are attributed to asymmetric and symmetric C-H stretching mode of aliphatic hydrocarbon chains. The broad band at 3275.08  $\text{cm}^{-1}$  represents the O-H stretching of the polyphenolic compounds, which is associated with strong hydrogen bonding [22]. These functional groups prove the existence of polyphenols in *Mentha piperita*, which might act as reducing and stabilizing agents in the CuO NPs synthesis.



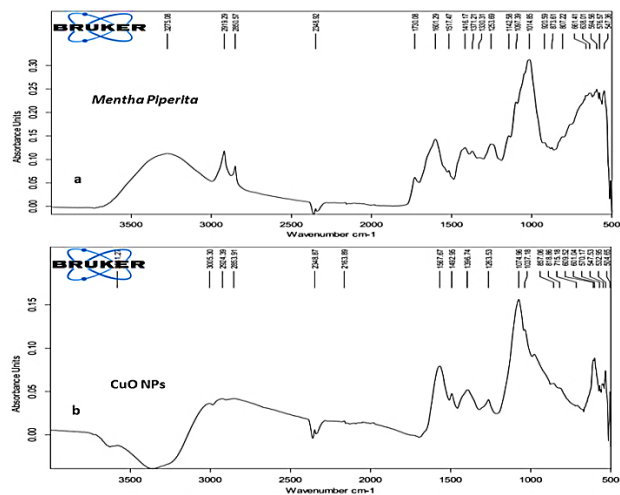


Fig. 3: IR Spectra of the dried *M. piperita* leaves and CuO NPs.

The FTIR spectra reveal that observed bands for functionalized CuO NPs (Fig.3b) are similar to those obtained for *Mentha piperita* (Fig.3a) with a slight shift, in addition to the absence of a carbonyl band near  $1700\text{ cm}^{-1}$ . Also, the band involving O-H vibration at  $3275.08\text{ cm}^{-1}$  of the polyphenols is shifted to  $3681.27\text{ cm}^{-1}$ . The shift of O-H vibration implies the involvement of the OH group in the reduction process. Further, the clear new absorption peaks at  $532.96\text{ cm}^{-1}$  and  $504.65\text{ cm}^{-1}$  are due to the Cu-O stretching vibration [23]. The significant changes of spectrum suggest the possible association of the polyphenolic compounds in the extract in the reduction process through the hydroxyl group and binding to the CuONPs through the carbonyl groups.

### 3.4 X-ray Diffraction (XRD)

The XRD pattern of the CuO NPs at room temperature (Figure 4) did not show distinct diffraction peaks, suggesting that plant polyphenols capped  $\text{Cu}^{2+}$  ions and changed the bond connections of  $\text{Cu}^{2+}$  in the precursor salt [24,25].

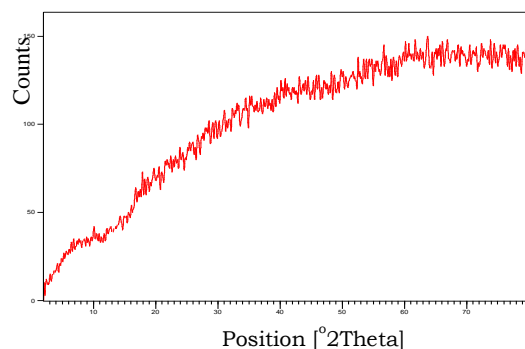


Fig. 4: X-ray diffraction pattern before calcination of CuO NPs.

The nanoparticles were annealed to enhance their crystallinity, and to decompose any extra compounds from the *Mentha piperita* extract that were not involved in the green synthesis process. Copper oxide nanoparticles were put in a ceramic boat and calcined in the furnace at  $600\text{ }^{\circ}\text{C}$  for 2 h. Figure 5 shows the XRD pattern of the calcined CuO NPs. The diffraction peaks were observed at  $2\theta$  values of  $33.19^{\circ}$ ,  $36.22^{\circ}$ ,  $39.40^{\circ}$ ,  $49.46^{\circ}$ ,  $58.92^{\circ}$ ,  $62.21^{\circ}$ ,  $66.91^{\circ}$ ,  $68.69^{\circ}$ ,  $73.02^{\circ}$ ,  $75.75^{\circ}$  corresponds to the lattice planes (110), (111), (200), (202), (020), (202), (113), (311), (220) and (400) respectively. XRD peaks are similar to the monoclinic structure of tenorite phase and well consistent with JCPDS card number 41-0254. The sharp and strong peak observed at  $36^{\circ}$  position with the plane (111) indicates that the sample has high crystalline quality. The Debye-Scherrer equation was used to calculate the average size of CuO NPs.

$$D = 0.94 \lambda / \beta \cos \theta$$

Where D is the particle's average crystallite size,  $\lambda$  is the X-ray radiation's wavelength (0.154 nm),  $\beta$  is the peak's full width at half

maximum (FWHM), and is the Bragg's angle of diffraction. CuO NPs were determined to have an average crystallite size of 42.51 nm.

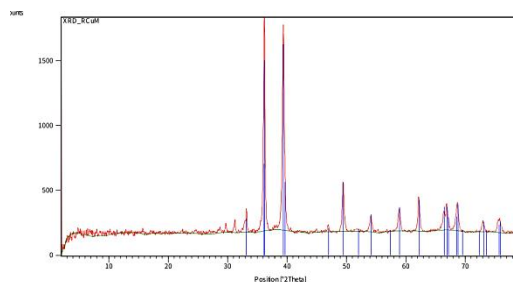


Fig. 5: X-ray diffraction pattern of CuO NPs after calcination at  $600\text{ }^{\circ}\text{C}$  for 2 h.

### 3.5 Scanning Electron Microscopy (SEM)

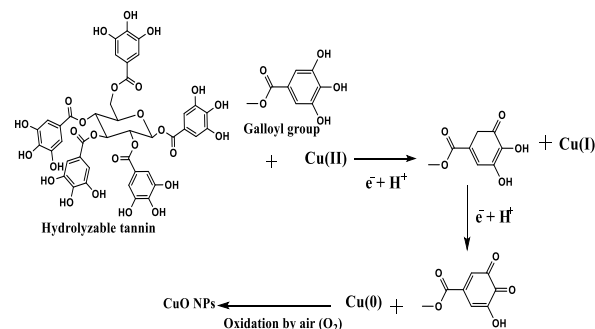
The surface morphology of the CuO nanoparticles was detected using SEM analysis. The SEM image of the CuO NPs is shown in Figure 6. As may be seen, the synthesized nanoparticles have spherical shape, as well as separated from each other and their structures were homogenous.



Fig. 6: SEM image of copper oxide nanoparticles

### 3.6 Plausible mechanism of CuO NPs synthesis

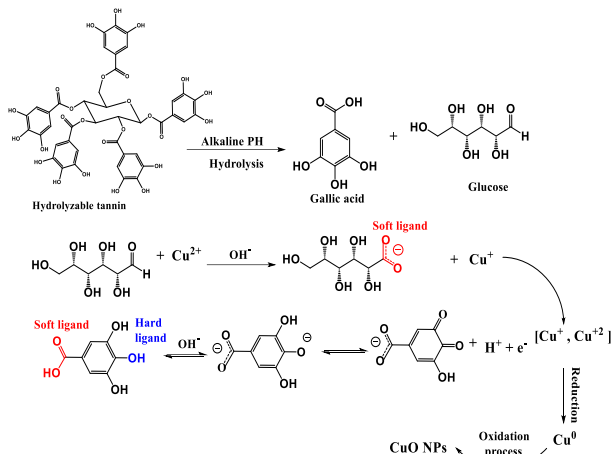
Although the mechanistic details of the biosynthesis processes are currently unclear, a range of mechanisms have been proposed to explain the formation of NPs. However, the exact mechanism of the synthesis process remains challenges, thus providing opportunities for further study. A proposed mechanism of the CuONPs synthesis from *Mentha piperita* is shown in scheme 1. The *Mentha piperita* leaf extract contains a high content of tannins (234.06 mg/g) with plenty of phenolic-OH of galloyl groups [21]. These functional groups can form a strong complex with  $\text{Cu}^{2+}$  ion. In the alkaline environment, the hydroxyl groups of polyphenolic compounds contained in the *Mentha piperita* extract are deprotonated and act to reduce the copper ions. The deprotonation of the hydroxyl groups was confirmed by the shift of O-H vibration of the polyphenols in the IR spectra. Accordingly, the copper ions oxidized the hydroxyl groups into carbonyl groups in the reduction reaction as  $\text{Cu}^{2+}$  is reduced to  $\text{Cu}^0$  NPs and subsequently oxidized by atmospheric oxygen to CuO NPs [26].



Scheme. 1 Reduction of Cu(II) ions by the galloyl groups of tannins of *Mentha piperita* leaf extract to produce CuO NPs

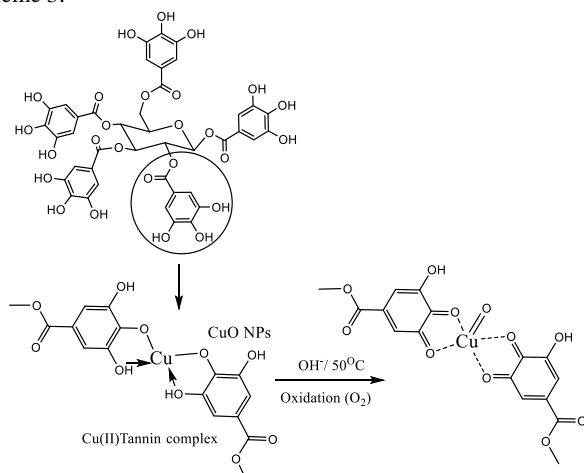
### 3.7 Stability of CuO nanoparticles in colloidal solution

The role of *Mentha piperita* in stabilizing CuO nanoparticles is considered as steric stabilization from the interaction between the possible functional groups of the polyphenols in the extract, the major ones being hydrolysable tannins, and Cu atoms on the surfaces. Tannins may be hydrolyzed by weak bases or weak acids to produce corresponding gallic acid and glucose moieties [27] scheme 2. Additionally, gallic acid and glucose in their anionic form are able to donate electrons (reducing power) and to transform into their quinone form. On the other hand, glucose is a known reducing agent, can only reduce  $\text{Cu}^{2+}$  to  $\text{Cu}^+$ , the resulting  $\text{Cu}^+$  is then converted to  $\text{Cu}^0$  by the anionic forms of the other hydrolyzed products scheme 2.



**Scheme. 2** A probable reaction mechanism for copper ions reduction using hydrolysable tannin.

The reduction and stabilization by the hydrolyzed products of tannins are also supported by the Hard Soft Acid Base (HSAB) principle. It has been previously indicated that hard ligands coordinate with the hard metals and soft ligands tend to coordinate with soft metals [28]. Based on the HSAB concept, the carbonyl group ( $\text{C}=\text{O}$ ) is a soft ligand while the hydroxyl group ( $-\text{OH}$ ) is a hard ligand in phenolic compounds as shown scheme 2. Thus, when the hard ligand ( $-\text{OH}$ ) in the hydrolyzed products of tannins comes in contact with the hard metal ion  $\text{Cu}^{2+}$  the formation of  $\text{Cu(II)}$ tannin complex will take place scheme 3.



**Scheme. 3** Plausible complexation and reduction of  $\text{Cu}^{2+}$  to CuO NPs.

When  $\text{Cu}^{2+}$  ions are reduced to  $\text{Cu}^0$ ,  $\text{Cu} (0)$  reacts with oxygen and spontaneously converts to the CuO NPs because of its high oxidation potential. In addition, the hydrolyzed products of tannins undergo oxidation resulting in the formation of their respective quinone forms. When the  $\text{C}=\text{O}$  soft ligand on quinone comes in contact with the surface of hard metals (CuO particles), the poor stabilization occurs. Hence, the carbonyl groups will be bound to CuO particles through electrostatic interactions. Accordingly, the possible active groups that are responsible for the stabilization CuO nanoparticles in an alkaline solution of *M. piperita* leaf extract should be phenolate anion

of galloyl groups, OH group of glucose and carboxylate group ( $\text{COO}^-$ ) of gallic acid Scheme 2. Furthermore, aggregation of nanoparticles is avoided by the presence of these free protecting agents [29]. The prevention of aggregation has been confirmed by the SEM image analysis.

#### 4. Conclusion

In summary, CuO nanoparticles were successfully prepared by reducing  $\text{Cu}^{2+}$  salt using the leaf extract of *Mentha piperita*. This method has many advantages over other reported methods, which include the availability of starting materials, low cost and easy experimental and use of toxic reagents is avoided. Moreover, the direct band gap value of CuO nanoparticles was small. Therefore, these CuO NPs may serve in applications such as semiconductor, catalyst and sensors. Calcinations process can effectively remove residue and lead to the better crystallization of CuO nanoparticles. The presence of phenolic-OH groups and ortho-dihydroxyphenyl groups in chemical structure of tannins are involved in the formation of complexes with  $\text{Cu}^{2+}$  ions and also take part in redox reactions. Also, in alkaline solution, the phenoxide anion of galloyl groups, carboxylate groups of gallic acid and hydroxyl group of glucose can strongly interact with the surface of CuO nanoparticles to supply the protection of the freshly made particles from aggregation.

#### Abbreviations

CuONPs: Copper oxide nanoparticles  
 SPR: Surface plasmon resonance  
 FT-IR: Fourier transform infrared spectroscopy  
 UV-VIS: Ultraviolet-visible spectroscopy  
 XRD: X-ray diffraction analysis  
 SEM: Scanning electron microscopy

#### Acknowledgements

Authors are grateful to the Department of Chemistry Zawia University, Petroleum Training & Qualifying Institute in Tripoli, Polymer Research Center in Tripoli, Libya and the National Center for Medical Research in Zawia for providing support towards this work. Authors also would like to thank Prof. Hussain Ibrahim Alarabi and Prof. Salem Khalifa Elfared (Chemistry Department, Zawia University) for their helpful discussions and advice during development of this work.

#### References

- [1]- Mohindru, J. J., Garg, U. K., (2017), Green synthesis of copper nanoparticles using tea leaf extract., *Int. J. Eng. Sci. Res. Technol.*, **6**(7), 307-311. DOI:10.5281/zenodo.827502
- [2]- Yip, S. K., and Sauls, J. A., (1992), Nonlinear Meissner effect in CuO superconductors., *Physical review letters.*, **69**(15), 2264-2267. DOI:10.1103/PhysRevLett.69.2264
- [3]- Sharma, J. K., Akhtar, M. S., Ameen, S., Srivastava, P., and Singh, G., (2015). Green synthesis of CuO nanoparticles with leaf extract of Calotropis gigantea and its dye-sensitized solar cells applications., *Journal of Alloys and Compounds.*, **632**, 321-325. DOI:10.1016/J.JALLCOM.2015.01.172
- [4]- Varghese, R., Prabu, H. J., and Johnson, I., (2017). Green Synthesis and Characterizations of Flower Shaped CuO Nanoparticles for Biodiesel Application., *Sensors & Transducers.*, **210**(3), 38-41. <http://www.sensorsportal.com>
- [5]- Manjari, G., Saran, S., Arun, T., Rao, A. V. B., and Devipriya, S. P., (2017). Catalytic and recyclability properties of phyto-genic copper oxide nanoparticles derived from Aglaia elaeagnoides flower extract., *Journal of Saudi Chemical Society.*, **21**(5), 610-618. DOI:10.1016/j.jscs.2017.02.004
- [6]- Pendashteh, A., Mousavi, M. F., and Rahmanifar, M. S., (2013). Fabrication of anchored copper oxide nanoparticles on graphene oxide nanosheets via an electrostatic coprecipitation and its application as supercapacitor., *Electrochimica Acta.*, **88**, 347-357. DOI:10.1016/j.electacta.2012.10.088
- [7]- Momeni, S., and Sedaghati, F., (2018). CuO/Cu<sub>2</sub>O nanoparticles: A simple and green synthesis, characterization and their electrocatalytic performance toward formaldehyde oxidation., *Microchemical Journal.*, **143**, 64-71. DOI:10.1016/j.microc.2018.07.035

- [8]- ThekkaePadil, V. V. T., Černík, M., (2013). Green synthesis of copper oxide nanoparticles using gum karaya as a biotemplate and their antibacterial application., *International journal of nanomedicine.*, **8**, 889-898. DOI:10.2147/IJN.S40599
- [9]- Wongpisutpaisan, N., Charoonsuk, P., Vittayakorn, N., and Pecharapa, W., (2011). Sonochemical synthesis and characterization of copper oxide nanoparticles., *Energy Procedia.*, **9**, 404-409. DOI:10.1016/egy.pro.2011.09.044
- [10]- Aparna, Y., Rao, K. E., and Subbarao, P. S., (2012). Synthesis and characterization of CuO nano particles by novel sol-gel method., In *Proceedings of the 2nd International Conference on Environment Science and Biotechnology*. DOI:10.7763/IPCBE.2012.V48.30
- [11]- Dar, M. A., Ahsanulhaq, Q., Kim, Y. S., Sohn, J. M., Kim, W. B., and Shin, H. S., (2009). Versatile synthesis of rectangular shaped nanobal-like CuO nanostructures by hydrothermal method; structural properties and growth mechanism., *Applied Surface Science.*, **255**(12), 6279-6284. DOI:10.1016/j.apsusc.2009.02.002
- [12]- Toboonsung, B., Singjai, P., (2011). Formation of CuO nanorods and their bundles by an electrochemical dissolution and deposition process., *Journal of Alloys and Compounds.*, **509**(10), 4132-4137. DOI:10.1016/j.jallcom.2010.12.180
- [13]- Guo, L., Tong, F., Liu, H., Yang, H., and Li, J., (2012). Shape-controlled synthesis of self-assembly cubic CuO nanostructures by microwave., *Materials Letters.*, **71**, 32-35. DOI:10.1016/j.matlet.2011.11.105.
- [14]- Dhineshababu, N. R., Rajendran, V., Nithyavathy, N., and Vetumperumal, R., (2016). Study of structural and optical properties of cupric oxide nanoparticles. *Applied Nanoscience.*, **6**(6), 933-939. DOI:10.1007/s13204-015-0499-2
- [15]- Zoolfakar, A. S., Rani, R. A., Morfa, A. J., O'Mullane, A. P., and Kalantar-Zadeh, K., (2014). Nanostructured copper oxide semiconductors: a perspective on materials, synthesis methods and applications., *journal of materials chemistry c.*, **2**(27), 5247-5270. DOI:10.1039/C4TC00345D
- [16]- Patil, S. R., Patil, R. S., and Godghate, A. G., (2016). Mentha piperita Linn: Phytochemical, antibacterial and dipterian adulticidal approach., *Int. J. Pharm. Pharm. Sci.*, **8**(3), 352-355. <https://innovareacademics.in/journals/index.php/ijpps/article/view/10370>.
- [17]- Dyab, A. S., Aly, A. M., and Matuk, H. I., (2015). Enhancement and Evaluation of Peppermint (Mentha Piperita L.) Beverage., *Life Sciences Research.*, **3**, 175-185. [www.researchpublish.com](http://www.researchpublish.com)
- [18]- Buazar, F., Sweidi, S., Badri, M., and Kroushawi, F., (2019). Biofabrication of highly pure copper oxide nanoparticles using wheat seed extract and their catalytic activity: A mechanistic approach. *Green Processing and Synthesis.*, **8**(1), 691-702. DOI: 10.1515/gps-2019-0040
- [19]- Qamar, H., Rehman, S., Chauhan, D. K., Tiwari, A. K., and Upmanyu, V., (2020). Green Synthesis, Characterization and Antimicrobial Activity of Copper Oxide Nanomaterial Derived from Momordica charantia., *International Journal of Nanomedicine.*, **15**, 2541-2553. DOI:10.2147/IJN.S240232
- [20]- Koshy, J., George, K. C., (2015). Annealing effects on crystallite size and band gap of CuO nanoparticles., *Int J Nanosci Nanotechnol.*, **6**(1), 1-8. <http://www.irphouse.com>
- [21]- Akhbari, M., Hajiaghaee, R., Ghafarzadegan, R., Hamed, S., and Yaghoobi, M., (2018). Process optimisation for green synthesis of zero-valent iron nanoparticles using Mentha piperita., *IET nanobiotechnology.*, **13**(2), 160-169. DOI:10.1049/iet-nbt.2018.5040
- [22]- Shtewi, F. A., Barag, W. M., & Tarroush, A. A., (2021). Green Synthesis and Characterization of Iron Oxide Nanoparticles Using Mentha Piperita Leaves Extract., *International Science and Technology Journal.*, **24**, 355-372. DOI:10.13140/RG.2.2.16073.36965
- [23]- Taghavi Fardood, S., Ramazani, A., (2016). Green synthesis and characterization of copper oxide nanoparticles using coffee powder extract., *Journal of Nanostructures.*, **6**(2), 167-171. DOI:10.7508/jns.2016.02.009
- [24]- Wang, Z., An, P., (2017). Characterization of Copper Complex Nanoparticles synthesized by Plant Polyphenols., *BioRxiv*. DOI: 10.1101/134940
- [25]- Barag, W. M., Shtewi, F. A., & Tarroush, A. A., (2021). Green Synthesis, Structural and Optical Properties of Copper Oxide Nanoparticles using Malva Parviflora. *Journal of Pure & Applied Sciences.*, **20**(1), 25-29. DOI: <https://doi.org/10.51984/jopas.v20i1.964>
- [26]- Siddiqi, K. S., Husen, A., (2020). Current status of plant metabolite-based fabrication of copper/copper oxide nanoparticles and their applications: a review., *Biomaterials Research.*, **24**(1), 1-15.
- [27]- Somchaidee, P., & Tedsree, K. (2018). Green synthesis of high dispersion and narrow size distribution of zero-valent iron nanoparticles using guava leaf (*Psidium guajava L*) extract. *Advances in Natural Sciences: Nanoscience and Nanotechnology*, **9**(3), 035006. DOI: 10.1088/2043-6254/aad5d7
- [28]- Eslami, S., Ebrahimzadeh, M. A., and Biparva, P., (2018). Green synthesis of safe zero valent iron nanoparticles by Myrtus communis leaf extract as an effective agent for reducing excessive iron in iron-overloaded mice, a thalassemia model. *RSC advances.*, **8**(46), 26144-26155. DOI: 10.1039/C8RA04451A
- [29]- Kumar, K. M., Mandal, B. K., and Tammina, S. K., (2013). Green synthesis of nano platinum using naturally occurring polyphenols., *RSC advances.*, **3**(12), 4033-4039. DOI:10.1039/C3RA22959A